

C.P. No. 1213



C.P. No. 1213

PROCUREMENT EXECUTIVE, MINISTRY OF DEFENCE

AERONAUTICAL RESEARCH COUNCIL

CURRENT PAPERS

Some Modifications to the Calculation
Method for Wings with Part-Span
Extending-Chord Flaps given in
RAE Technical Report 69034

by

J. McKie

Aerodynamics Dept., R.A.E., Farnborough

LONDON: HER MAJESTY'S STATIONERY OFFICE

1972

PRICE 60 p NET

UDC 533.693.1 : 533.6.048.1 : 533.694.511 : 533.6.011.32 : 533.6.013.13 :
533.6.013.127

CP No.1213*
September 1971

SOME MODIFICATIONS TO THE CALCULATION METHOD FOR WINGS WITH
PART-SPAN EXTENDING-CHORD FLAPS GIVEN IN RAE TECHNICAL REPORT 69034

by
J. McKie

SUMMARY

A method is given for the approximate solution of a version of Prandtl's aerofoil equation for wings with an arbitrary number of discontinuities in chord or geometric angle of incidence. The method is an attempt to improve on an earlier one given in RAE Technical Report 69034. For the example of a swept wing of large aspect ratio with part-span, extending-chord flaps, the results for lift, drag and vortex-drag factor by the improved method show no significant differences from those calculated by the earlier method. Comments are made on other factors affecting the accuracy of the solution.

* Replaces RAE Technical Report 71201 - ARC 33547

CONTENTS

| | <u>Page</u> |
|---|-------------|
| 1 INTRODUCTION | 3 |
| 2 ANALYSIS FOR EXTRA COLLOCATION POINTS | 4 |
| 3 SOLUTION WITH DISCONTINUITIES | 12 |
| 4 RESULTS | 16 |
| 5 CONCLUSIONS | 19 |
| Acknowledgement | 19 |
| Tables 1-3 | 20 |
| Symbols | 22 |
| References | 24 |
| Illustrations | Figures 1-9 |
| Detachable abstract cards | |

1 INTRODUCTION

The RAE Standard Method¹, for the calculation of loadings on swept wings, divides the vorticity distribution on the wing into chordwise and spanwise distributions. It is implied that the downwash induced by the chordwise and trailing vorticity is constant over the chord of the wing. This enables the spanwise loading to be determined from an integral equation, which is a form of Prandtl's classical aerofoil equation, modified to include sweepback and small-aspect-ratio effects.

The customary way of solving this equation is by Multhopp's approximate method of quadrature², which uses a Fourier technique. This demands that chord, local lift slope and local angle of incidence are all continuous across the span of the wing. Multhopp gave a modified solution² for the case of discontinuities in the distribution of angle of incidence, and Weissinger has extended this to include a single discontinuity in chord³. Weber⁴ has adapted this method to make it suitable for swept wings of small aspect ratio, by allowing the downwash factor and the sectional lift slope to vary across the span of the wing. The approximation for the spanwise loading was chosen in such a manner that the calculation of its values at the Multhopp collocation points was not affected by defining it at the additional point.

For wings with part-span, extending-chord flaps, there will usually be more than one discontinuity in chord and angle of incidence. An approximate way of dealing with this situation has been given by the author⁵. It was supposed that the calculation could be carried out in an analogous manner to that for the case of a single additional point. That is, the defining of the loading at the additional points did not affect the calculation of the spanwise load distribution at the Multhopp collocation points.

This Report describes a method whereby this assumption is removed and the effect of the necessity of defining the loading at the extra points is taken properly into account. An approximation for the spanwise loading has been chosen which retains the Weber solution⁴ as a special case for a single extra point with a possible discontinuity in chord or angle of incidence. With the former kind of discontinuity, the magnitude of the jump in the induced angle of incidence depends on the value of the loading at the discontinuity. It is, therefore, important to find a good approximation to the loading at all the additional points. In the next section, the solution of the spanwise loading equation will be extended to include any number of extra collocation points,

whose spanwise position is arbitrary. In section 3, the results of the analysis will be applied to the situation where discontinuities in chord and twist occur at these extra points. The new method has been programmed for a computer, and in section 4 a comparison is made with the results of the earlier method, for a typical wing.

2 ANALYSIS FOR EXTRA COLLOCATION POINTS

The nondimensional spanwise loading $\gamma(\eta)$ is given by the equation

$$\gamma(\eta) = \frac{a(\eta)c(\eta)}{2b} [\alpha(\eta) - \omega\alpha_{i0}(\eta)] \quad (1)$$

The induced angle of incidence $\omega\alpha_{i0}(\eta)$ is determined by the trailing vorticity, which is itself a function of the spanwise load distribution. Hence $\gamma(\eta)$ can be found as a solution of the integral equation:-

$$\frac{2b}{a(\eta)c(\eta)} \gamma(\eta) = \alpha(\eta) - \frac{\omega}{2\pi} \int_{-1}^{+1} \frac{d\gamma(\xi)}{d\xi} \frac{d\xi}{\eta - \xi} \quad (2)$$

In these equations, η or ξ is the spanwise coordinate, ± 1 at the wing tips, $a(\eta)$ is the local lift slope, $c(\eta)$ the local wing chord, and $\alpha(\eta)$ the local geometric angle of incidence. Multhopp solved equation (2) approximately², by using an interpolation function

$$\bar{\gamma}(\vartheta) = \frac{2}{m+1} \sum_{n=1}^m \gamma_n \sum_{\mu=1}^m \sin \mu\vartheta_n \sin \mu\vartheta \quad (3)$$

where $\eta = \cos \vartheta$ and $\gamma_n = \gamma(\vartheta_n)$, $\vartheta_n = \frac{n\pi}{m+1}$. At the m collocation points ϑ_v (the Multhopp points), which are equispaced with respect to the ϑ coordinate, $\bar{\gamma}(\vartheta_v) = \gamma_v$.

Equation (3) enables an approximate value of γ to be found at any point on the span of the wing. However, if there are discontinuities in chord at k extra points ϑ_s , which are distributed arbitrarily across the span, then it is desirable to find the values of the loading $\gamma(\eta)$ at these points by a better approximation than is given by equation (3). A solution to equation (2) will be sought, of the form

$$\gamma(\vartheta) = \bar{\gamma}(\vartheta) + \sin(\overline{m+1}\vartheta) \sum_{r=1}^k a_r \cos(\overline{r-1}\vartheta) \quad (4)$$

where the coefficients a_r are to be found. The second term on the right-hand side vanishes at a Multihopp point, i.e.

$$\gamma(\vartheta_v) = \bar{\gamma}(\vartheta_v) = \gamma_v$$

so that it could be considered as a 'correction' to the first approximation $\bar{\gamma}$. At the extra points

$$\gamma(\vartheta_s) = \bar{\gamma}(\vartheta_s) + \sin(\overline{m+1}\vartheta_s) \sum_{r=1}^k a_r \cos(\overline{r-1}\vartheta_s) .$$

Thus the unknown coefficients a_r can be expressed

$$\{a\} = \Psi^{-1} \{\gamma_s - \bar{\gamma}_s\} \quad (5)$$

where Ψ is a square matrix of order k with the (s,r) element

$$\sin(\overline{m+1}\vartheta_s) \cos(\overline{r-1}\vartheta_s)$$

and $\{a\}$, $\{\gamma_s - \bar{\gamma}_s\}$ are column vectors of dimension k . Note that if one of the extra points coincides with a Multihopp point, i.e. $\vartheta_s = \vartheta_n$, then $\{\gamma_s - \bar{\gamma}_s\}$ has a null element and Ψ a row of zeros in the corresponding position. In this case Ψ^{-1} is singular and $\{a\}$ arbitrary. Consequently, either a reduced set of equations should be used (this particular η_s is dropped), or the set ϑ_v must be changed by altering the value of m .

The induced angle of incidence can be written

$$\alpha_{io}(\vartheta) = \frac{1}{2\pi} \int_0^\pi \frac{d\gamma}{d\vartheta'} \frac{d\vartheta'}{\cos \vartheta' - \cos \vartheta} .$$

If the approximate form of $\gamma(\vartheta)$ given by equation (4) is substituted into this expression, then

$$\alpha_{10}(\vartheta) = \frac{1}{2\pi} \int_0^\pi \frac{d\bar{\gamma}}{d\vartheta'} \frac{d\vartheta'}{\cos \vartheta' - \cos \vartheta} + \frac{1}{4} \sum_{r=1}^k a_r \left\{ (m+r) \frac{\sin(\overline{m+r\vartheta})}{\sin \vartheta} + (m+2-r) \frac{\sin(\overline{m+2-r\vartheta})}{\sin \vartheta} \right\}$$

where use has been made of the Glauert integral

$$\int_0^\pi \frac{\cos n\vartheta}{\cos \vartheta - \cos \varphi} d\vartheta = \pi \frac{\sin n\varphi}{\sin \varphi} .$$

An expression for $\bar{\gamma}$ has been given in equation (3). Hence the induced angle of incidence may be expressed in terms of γ_n , the spanwise loading at the Multhopp points, and the coefficients a_r which are yet to be determined.-

$$\begin{aligned} \alpha_{10}(\vartheta) &= \sum_{n=1}^m \gamma_n \frac{1}{(m+1) \sin \vartheta} \sum_{\mu=1}^m \mu \sin \mu\vartheta_n \sin \mu\vartheta + \\ &+ \frac{1}{4} \sum_{r=1}^k a_r \left\{ \frac{2(m+1) \sin(\overline{m+1\vartheta}) \cos(\overline{r-1\vartheta})}{\sin \vartheta} \right\} + \\ &+ \frac{1}{4} \sum_{r=1}^k a_r \left\{ \frac{2(r-1) \cos(\overline{m+1\vartheta}) \sin(\overline{r-1\vartheta})}{\sin \vartheta} \right\} . \end{aligned}$$

At the Multhopp points η_v

$$\sin(\overline{m+1\vartheta}_v) = 0 \quad \text{and} \quad \cos(\overline{m+1\vartheta}_v) = (-1)^v .$$

Thus at these points, the induced angle of incidence reduces to

$$\alpha_{10}(\vartheta_v) = b_{vv} \gamma_v - \sum' b_{vn} \gamma_n + \frac{1}{2} \frac{(-1)^v}{\sin \vartheta_v} \sum_{r=1}^k a_r (r-1) \sin(\overline{r-1\vartheta}_v) . \quad (6)$$

Here, b_{vv} and b_{vn} are the usual Multhopp coefficients² and \sum' denotes summation over all n except $n = v$. If there is only a single extra collocation point, then the last term in equation (6) is zero, and the Weber⁴ result is achieved, that the calculation of γ at the position η_v is unaffected by its calculation for the additional point η_s . For more than one extra collocation point,

equation (6) indicates that if the spanwise load distribution is approximated by the function (4), then the loading γ_s at these extra points has to be taken into account when determining the loading at the Multhopp points.

At the additional points η_s , the equation for the induced angle of incidence becomes

$$\begin{aligned} \alpha_{io}(\vartheta_s) = & \sum_{n=1}^m \gamma_n \frac{1}{(m+1) \sin \vartheta_s} \sum_{\mu=1}^m \mu \sin \mu \vartheta_n \sin \mu \vartheta_s + \\ & + \frac{m+1}{2} \frac{\sin(\overline{m+1} \vartheta_s)}{\sin \vartheta_s} \sum_{r=1}^k a_r \cos(\overline{r-1} \vartheta_s) + \\ & + \frac{\cos(\overline{m+1} \vartheta_s)}{2 \sin \vartheta_s} \sum_{r=1}^k a_r (r-1) \sin(\overline{r-1} \vartheta_s) . \end{aligned}$$

The second term on the right-hand side above may be replaced by (see equation (4))

$$\frac{m+1}{2 \sin \vartheta_s} [\gamma(\vartheta_s) - \bar{\gamma}(\vartheta_s)]$$

which, on substitution for $\bar{\gamma}$ from equation (3), becomes

$$\frac{m+1}{2 \sin \vartheta_s} \gamma_s - \frac{1}{\sin \vartheta_s} \sum_{n=1}^m \gamma_n \sum_{\mu=1}^m \sin \mu \vartheta_n \sin \mu \vartheta_s .$$

Thus at the extra collocation points η_s , the induced angle of incidence may be written

$$\alpha_{io}(\vartheta_s) = b_{ss} \gamma_s - \sum_{n=1}^m b_{sn} \gamma_n + \frac{\cos(\overline{m+1} \vartheta_s)}{2 \sin \vartheta_s} \sum_{r=1}^k a_r (r-1) \sin(\overline{r-1} \vartheta_s) \quad (7)$$

where the coefficients b_{ss} and b_{sn} are those given by Weber⁴:-

$$b_{ss} = \frac{m+1}{2 \sin \vartheta_s}$$

$$\begin{aligned} b_{sn} &= \frac{1}{(m+1) \sin \vartheta_s} \sum_{\mu=1}^m (m+1-\mu) \sin \mu \vartheta_n \sin \mu \vartheta_s \\ &= \frac{a_{sn} \sin \vartheta_n}{(m+1)(\cos \vartheta_s - \cos \vartheta_n)^2} \end{aligned}$$

$$a_{sn} = \begin{cases} \left[\sin \left(\frac{m+1}{2} \vartheta_s \right) \right]^2 & n \text{ even} \\ \left[\cos \left(\frac{m+1}{2} \vartheta_s \right) \right]^2 & n \text{ odd} \end{cases}$$

If there is only one extra point, then the last term of (7) is zero. Hence Weber's result⁴ is retained as the special case of $k=1$.

A major task now is to determine the coefficients a_r . Consider the value of the approximation $\bar{\gamma}$ at η_s , then from (3)

$$\bar{\gamma}_s = \frac{2}{m+1} \sum_{n=1}^m \gamma_n \sum_{\mu=1}^m \sin \mu \vartheta_n \sin \mu \vartheta_s \quad (8)$$

Write

$$\begin{aligned} T &= \sum_{\mu=1}^m \sin \mu \vartheta_n \sin \mu \vartheta_s \\ &= \frac{1}{2} \sum_{\mu=1}^m \cos \mu(\vartheta_n - \vartheta_s) - \frac{1}{2} \sum_{\mu=1}^m \cos \mu(\vartheta_n + \vartheta_s) \end{aligned}$$

Now

$$\sum_{\mu=1}^m \cos \mu \phi = \Re \sum_{\mu=1}^m e^{i\mu\phi} = \Re \sum_{\mu=1}^m z^\mu$$

where 'Re' means the real part of a complex expression and $z = e^{i\phi}$.

Therefore

$$\begin{aligned} \sum_{\mu=1}^m \cos \mu\phi &= \text{Re} \left[\frac{1 - z^{m+1}}{1 - z} - 1 \right] \\ &= \frac{\sin \phi \sin (m+1)\phi}{2(1 - \cos \phi)} - \frac{1 + \cos (m+1)\phi}{2} \end{aligned}$$

Thus the sum T can be written

$$\begin{aligned} T &= \frac{1}{4} \left\{ \frac{\sin (\vartheta_n - \vartheta_s) \sin (m+1 \cdot \overline{\vartheta_n - \vartheta_s})}{[1 - \cos (\vartheta_n - \vartheta_s)]} - \frac{\sin (\vartheta_n + \vartheta_s) \sin (m+1 \cdot \overline{\vartheta_n + \vartheta_s})}{[1 - \cos (\vartheta_n + \vartheta_s)]} \right\} - \\ &\quad - \frac{1}{4} \{ \cos (m+1 \cdot \overline{\vartheta_n - \vartheta_s}) - \cos (m+1 \cdot \overline{\vartheta_n + \vartheta_s}) \} \end{aligned}$$

therefore

$$\begin{aligned} T &= - \frac{(-1)^n}{4D} \sin (m+1\vartheta_s) \{ \sin (\vartheta_n - \vartheta_s) + \sin (\vartheta_n + \vartheta_s) - \sin (\vartheta_n - \vartheta_s) \cos (\vartheta_n + \vartheta_s) \\ &\quad - \sin (\vartheta_n + \vartheta_s) \cos (\vartheta_n - \vartheta_s) \} \end{aligned}$$

$$\text{where } D = [1 - \cos (\vartheta_n - \vartheta_s)] [1 - \cos (\vartheta_n + \vartheta_s)] = [\cos \vartheta_n - \cos \vartheta_s]^2$$

therefore

$$T = (-1)^n \frac{\sin (m+1\vartheta_s) \sin \vartheta_n}{2(\cos \vartheta_n - \cos \vartheta_s)}$$

Hence equation (8) may be written

$$\bar{\gamma}_s = \sum_{n=1}^m c_{sn} \gamma_n \quad (9)$$

where the $m \times k$ coefficients c_{sn} are given by

$$c_{sn} = \frac{(-1)^n \sin (m+1\vartheta_s) \sin \vartheta_n}{m+1 \cos \vartheta_n - \cos \vartheta_s} \quad (10)$$

If ϑ_s coincides with one of the Multhopp points ϑ_v , then the coefficients c_{sn} which, in equation (9), multiply the values of γ at all the other Multhopp points, are zero. To examine the value of c_{sv} , suppose $\vartheta_s = \vartheta_v + \varepsilon$, where ε is small.

$$c_{sv} = \frac{(-1)^v}{m+1} \frac{(-1)^v \sin \varepsilon(m+1) \sin \vartheta_v}{[\cos \vartheta_v - \cos \vartheta_v \cos \varepsilon + \sin \vartheta_v \sin \varepsilon]}$$

Then as ε tends to zero

$$\lim_{\varepsilon \rightarrow 0} c_{sv} = \lim_{\varepsilon \rightarrow 0} \frac{\varepsilon(m+1) \sin \vartheta_v}{(m+1)[\cos \vartheta_v \varepsilon^2/2 + \varepsilon \sin \vartheta_v]} = 1$$

Thus as $\vartheta_s \rightarrow \vartheta_v$, the only term remaining on the right-hand side of equation (9) is γ_v , i.e. $\bar{\gamma}_s \rightarrow \gamma_v$ which is as it should be.

Having now determined the values of $\bar{\gamma}$ at the additional collocation points in terms of γ_n , equation (4) enables γ_s to be written in terms of γ_n and the coefficients a_r :-

$$\gamma_s = \sum_{n=1}^m c_{sn} \gamma_n + \sin(\overline{m+1}\vartheta_s) \sum_{r=1}^k a_r \cos(\overline{r-1}\vartheta_s)$$

Consequently, equation (5) for the functions a_r can be rewritten as a function of the spanwise loading γ at both the Multhopp and extra collocation points (in matrix notation):-

$$\{a\} = \Psi^{-1} \{\Upsilon_s - \Gamma \Upsilon_v\} \quad (11)$$

where Υ_s is a column vector of dimension k , with elements γ_s

Υ_v is a column vector of dimension m , with elements γ_v

Γ is a rectangular matrix of order $k \times m$, with elements $-c_{sn}$.

Equation (4) can now no longer be used to define γ_s in terms of known quantities. However, equation (1) provides a better approximation, as it involves the known quantities of chord, lift slope and geometric angle of incidence, and only the induced angle of incidence must be estimated. Hence

$$\gamma_s = \frac{a(\eta_s)c(\eta_s)}{2b} [\alpha(\eta_s) - \omega\alpha_{i_0}(\eta_s)] .$$

In this equation, the values of the induced angle of incidence can be found from equation (7), which in matrix form is:-

$$\{\alpha_{i_0_s}\} = \mathcal{R}_3 \Upsilon_s - \mathcal{R}_4 \Upsilon_v + M_s \{a\} .$$

Similarly, for the values at the Multihopp points

$$\{\alpha_{i_0_v}\} = \mathcal{R}_1 \Upsilon_v - \mathcal{R}_2 \Upsilon_s + M_v \{a\}$$

where $\{\alpha_{i_0_v}\}$ is a column vector of dimension m , with elements $\alpha_{i_0_v}$
 $\{\alpha_{i_0_s}\}$ " " " " " " " " k , " " $\alpha_{i_0_s}$
 \mathcal{R}_1 " " diagonal matrix of order $m \times m$, " " b_{vv}
 \mathcal{R}_2 " " square " " " " $m \times m$, " " b_{vn}
 \mathcal{R}_3 " " diagonal " " " " $k \times k$, " " b_{ss}
 \mathcal{R}_4 " " rectangular " " " " $k \times m$, " " b_{sn}
 M_v " " " " " " " " $m \times k$,
 with (n,s) element $\frac{1}{2}(-1)^n (s-1) \frac{\sin(\overline{s-1}\vartheta_n)}{\sin \vartheta_n}$
 M_s is a square matrix of order $k \times k$,
 with (s,r) element $\frac{1}{2}(r-1) \frac{\sin(\overline{r-1}\vartheta_s) \cos(\overline{m+1}\vartheta_s)}{\sin \vartheta_s}$.

The vector of a_r may be removed by substitution from equation (11), so that the equation for the induced angle of incidence may finally be written in terms of Υ_v and Υ_s :-

$$\{\alpha_{i_0_v}\} = [\mathcal{R}_1 - \mathcal{R}_2 - M_v \Psi^{-1} \Gamma] \Upsilon_v + M_v \Psi^{-1} \Upsilon_s \quad (12)$$

$$\{\alpha_{i_0_s}\} = -[\mathcal{R}_4 + M_s \Psi^{-1} \Gamma] \Upsilon_v + [\mathcal{R}_3 + M_s \Psi^{-1} \Gamma] \Upsilon_s . \quad (13)$$

3 SOLUTION WITH DISCONTINUITIES

Suppose that at each of the points η_s discontinuities exist in either the chord c or the angle of incidence α , or both. Then the induced angle of incidence at these points will also be discontinuous and the normal Fourier analysis method of solution for γ_v , γ_s cannot be carried out - equation (13) is not meaningful. The Multhopp-Weissinger-Weber method considers this situation by dividing the loading γ into two parts:-

$$\gamma(\eta) = \gamma_I(\eta) + \gamma^*(\eta) \quad . \quad (14)$$

Both $\gamma_I(\eta)$ and $\gamma^*(\eta)$ are continuous; the former depends on the positions and amounts of the discontinuities, the latter depends on a continuous distribution of angle of incidence. $\gamma_I(\eta)$ is a specially chosen analytic function which produces a discontinuous distribution of angle of incidence $\alpha_{I0}(\eta)$. $\gamma^*(\eta)$ is an approximate function of the form described in the previous section, which induces a continuous distribution of angle of incidence $\alpha_{i0}^*(\eta)$.

Consider the discontinuity point η_s , where there occurs a jump in geometric angle of incidence of amount σ_s , i.e.

$$\sigma_s = \alpha(\eta_s + 0) - \alpha(\eta_s - 0) \quad (15)$$

and also a jump in wing chord. Define

$$\tau_s = \frac{2b}{a(\eta_s)} \left[\frac{1}{c(\eta_s - 0)} - \frac{1}{c(\eta_s + 0)} \right] \quad . \quad (16)$$

The spanwise loading $\gamma(\eta)$ must be continuous, hence at η_s

$$\begin{aligned} \gamma(\eta_s + 0) &= \gamma(\eta_s - 0) = \gamma_s \\ &= \frac{a(\eta_s)c(\eta_s + 0)}{2b} [\alpha(\eta_s + 0) - \omega\alpha_{i0}(\eta_s + 0)] \\ &= \frac{a(\eta_s)c(\eta_s - 0)}{2b} [\alpha(\eta_s - 0) - \omega\alpha_{i0}(\eta_s - 0)] \quad . \end{aligned}$$

Consequently, at the discontinuity point η_s there occurs a jump in the value of the induced angle of incidence:-

$$\alpha_{i0}(\eta_s + 0) - \alpha_{i0}(\eta_s - 0) = \frac{\tau_s \gamma_s + \sigma_s}{\omega} \quad . \quad (17)$$

If the function $F(\vartheta, \vartheta_s)$ is defined as follows (see Multhopp²):-

$$F(\vartheta, \vartheta_s) = \frac{2}{\pi} \left[(\cos \vartheta - \cos \zeta) \ln \left(\frac{\sin \frac{1}{2}(\vartheta + \zeta)}{\sin \frac{1}{2}|\vartheta - \zeta|} \right) + \zeta \sin \vartheta \right]_{\zeta=\vartheta_s}^{\zeta=\pi} \quad (18)$$

then the load distribution $\gamma_I(\eta)$ formed by

$$\gamma_I(\vartheta) = \sum_{s=1}^k \frac{\gamma_s \tau_s + \bar{\sigma}_s}{\omega} F(\vartheta, \vartheta_s) \quad (19)$$

produces a discontinuous distribution of induced angle of incidence $\alpha_{ioI}(\vartheta)$ with a jump at each discontinuity of the required amount.

$$\alpha_{ioI}(\vartheta) = \begin{cases} 0 & \text{for } 0 \leq \vartheta < \vartheta_{s_1} \\ (\tau_1 \gamma_{s_1} + \sigma_1) / \omega_{s_1} & \vartheta_{s_1} < \vartheta < \vartheta_{s_2} \\ \text{"} + (\tau_2 \gamma_{s_2} + \sigma_2) / \omega_{s_2} & \vartheta_{s_2} < \vartheta < \vartheta_{s_3} \\ \text{etc.} & \end{cases} \quad (20)$$

Corresponding to the load distribution γ^* is the distribution of induced angle of incidence α_{io}^* , so that γ^* can be written

$$\gamma^*(\eta) = \frac{a(\eta)c(\eta)}{2b} \left[\alpha(\eta) - \omega \alpha_{ioI}(\eta) - \frac{2b}{a(\eta)c(\eta)} \gamma_I(\eta) - \omega \alpha_{io}^*(\eta) \right] \quad (21)$$

where $\gamma_I(\eta)$ is defined by equation (19) and $\alpha_{ioI}(\eta)$ by (20). From equations (12) and (13), α_{io}^* at the points η_v and η_s is given by

$$\begin{aligned} \{\alpha_{io_v}^*\} &= [\mathcal{R}_1 - \mathcal{R}_2 - M_v \Psi^{-1} \Gamma] \Upsilon_v^* + M_v \Psi^{-1} \Upsilon_s^* \\ \{\alpha_{io_s}^*\} &= [-\mathcal{R}_4 - M_s \Psi^{-1} \Gamma] \Upsilon_v^* + [\mathcal{R}_3 + M_s \Psi^{-1}] \Upsilon_s^* \end{aligned}$$

where Υ_v^* is a column vector of the m values of γ^* at the η_v positions, and Υ_s^* the vector of values at the k discontinuity points η_s . These two equations may be substituted into matrix equivalents of equation (21), so that at the Multhopp points there results:-

$$[\mathcal{R}_1 - \mathcal{R}_2 - M_v \Psi^{-1} \Gamma + N_v] \Upsilon_v^* = \Lambda_v - A_{i0_{Iv}} - M_v \Psi^{-1} \Upsilon_s^* - N_v \Upsilon_{Iv} \quad (22)$$

In this equation,

Λ_v is a column vector of dimension m , with elements $[\alpha/\omega]_v$

$A_{i0_{Iv}}$ is a column vector of dimension m , with elements $\begin{bmatrix} \alpha_{i0_I} \end{bmatrix}_v$

N_v is a diagonal matrix of order $m \times m$ with elements $\begin{bmatrix} 2b \\ \omega ac \end{bmatrix}_v$.

For the discontinuity points η_s , there is a choice of evaluating equation (21) at either side of the discontinuity: the $(\eta_s - 0)$ alternative is chosen here.

Thus on substituting for $\{\alpha^*\}_{i0_s}$:-

$$[\mathcal{R}_3 + M_s \Psi^{-1} + N_s] \Upsilon_s^* = \Lambda_s - A_{i0_{Is}} + [\mathcal{R}_4 + M_s \Psi^{-1} \Gamma] \Upsilon_v^* - N_s \Upsilon_{Is} \quad (23)$$

where Λ_s is a column vector of dimension k , with elements $[\alpha/\omega]_{s-}$

$A_{i0_{Is}}$ is a column vector of dimension k , with elements $\begin{bmatrix} \alpha_{i0_I} \end{bmatrix}_{s-}$

N_s is a diagonal matrix of order $k \times k$ with elements $\begin{bmatrix} 2b \\ \omega ac \end{bmatrix}_{s-}$.

The $(m + k)$ equations (22) and (23) are coupled via Υ_v^* , and through α_{i0_I} and Υ_I , which are both functions of Υ_s^* . Υ_I is expressed in terms of Υ by equation (19), which becomes in matrix notation

$$\Upsilon_{Iv} = \mathcal{F}_v [\mathcal{L}_1 \Upsilon_s + \mathcal{L}_2]$$

$$\Upsilon_{Is} = \mathcal{F}_s [\mathcal{L}_1 \Upsilon_s + \mathcal{L}_2]$$

so that by equation (14),

$$\Upsilon_{Is} = [\mathcal{J} - \mathcal{F}_s \mathcal{L}_1]^{-1} \mathcal{F}_s [\mathcal{L}_1 \Upsilon_s^* + \mathcal{L}_2] \quad (24)$$

$$\Upsilon_{Iv} = \mathcal{F}_v \mathcal{L}_1 [\mathcal{J} - \mathcal{F}_s \mathcal{L}_1]^{-1} \Upsilon_s^* + \mathcal{F}_v [\mathcal{L}_1 (\mathcal{J} - \mathcal{F}_s \mathcal{L}_1)^{-1} \mathcal{F}_s + \mathcal{J}] \mathcal{L}_2 \quad (25)$$

In these equations

| | | | | | |
|-----------------|----------------------------------|--------------|---------------|---------------------|---|
| \mathcal{F}_v | is a rectangular matrix of order | $m \times k$ | with | (v,t) element | $F(\vartheta_v, \vartheta_t)$ |
| \mathcal{F}_s | " " square | " " " | " | $k \times k$ | " (s,t) " $F(\vartheta_s, \vartheta_t)$ |
| \mathcal{J} | " " unit | " " " | " | " | " |
| ℓ_1 | " " diagonal | " " " | " | " | elements $[\tau/\omega]_s$ |
| ℓ_2 | " " column vector of dimension | k | with elements | $[\sigma/\omega]_s$ | . |

The loading Υ_{Iv} can now be eliminated from equation (22) thus

$$[\mathcal{R}_1 - \mathcal{R}_2 + N_v - M_v \Psi^{-1} \Gamma] \Upsilon_v^* = \{ \Lambda_v - N_v \mathcal{F}_v (\ell_1 (\mathcal{J} - \mathcal{F}_s \ell_1)^{-1} \mathcal{F}_s + \mathcal{J}) \ell_2 \} - [M_v \Psi^{-1} + N_v \mathcal{F}_v \ell_1 (\mathcal{J} - \mathcal{F}_s \ell_1)^{-1}] \Upsilon_s^* - A_{io_{Iv}} \quad (26)$$

The vector $A_{io_{Iv}}$ is dependent on ℓ_1 , ℓ_2 and Υ_s^* through equations (20) and (24), and the particular geometric relationship between the discontinuity points η_s and the Multhopp points η_v . Thus equation (26) represents m simultaneous equations for the loading Υ_v^* expressed in terms of Υ_s^* and geometric terms only.

At the discontinuity points η_s , the angle of incidence induced by the loading Υ_I may easily be expressed as a function of Υ_s in matrix notation:-

$$A_{io_{Is}} = \mathcal{J}_2 \{ \ell_1 \Upsilon_s + \ell_2 \}$$

where \mathcal{J}_2 is a $k \times k$ square matrix formed from the unit matrix by making all lower left elements unity. By adding Υ_s^* to either side of equation (24)

$$\Upsilon_s = [\mathcal{J} - \mathcal{F}_s \ell_1]^{-1} [\Upsilon_s^* + \mathcal{F}_s \ell_2]$$

therefore

$$A_{io_{Is}} = \mathcal{J}_2 \ell_1 [\mathcal{J} - \mathcal{F}_s \ell_1]^{-1} \Upsilon_s^* + \mathcal{J}_2 \{ \ell_1 (\mathcal{J} - \mathcal{F}_s \ell_1)^{-1} \mathcal{F}_s + \mathcal{J} \} \ell_2 \quad .$$

If this is substituted back into equation (23), then

$$[\mathcal{R}_3 + (N_s + \mathcal{J}_2 \ell_1) (\mathcal{J} - \mathcal{F}_s \ell_1)^{-1} + M_s \Psi^{-1} \Gamma] \Upsilon_s^* = [\mathcal{R}_4 + M_s \Psi^{-1} \Gamma] \Upsilon_v^* + (\Lambda_s - \mathcal{J}_2 \ell_2) - (\mathcal{J}_2 \ell_1 + N_2) (\mathcal{J} - \mathcal{F}_s \ell_1)^{-1} \mathcal{F}_s \ell_2 \quad (27)$$

Equations (26) and (27) form a set of $m + k$ linear, simultaneous, algebraic equations for the unknowns Γ_v^* and Γ_s^* . They may be solved by an iterative process. Initially, assume Γ_s^* to be zero, and solve equation (26) for the m values of Γ_v^* . These are then substituted into equation (27), which is solved to obtain a first estimate of Γ_s^* . This is used to obtain a second set of Γ_v^* from (26), and the cycle repeated till a consistent set of values Γ^* is found. The spanwise loading Γ then follows from

$$\Gamma_s = (\mathcal{J} - \mathcal{J}_s \ell_1)^{-1} \Gamma_s^* + (\mathcal{J} - \mathcal{J}_s \ell_1)^{-1} \mathcal{J}_s \ell_2 \quad (28)$$

$$\Gamma_v = \Gamma_v^* + \mathcal{J}_v \ell_1 (\mathcal{J} - \mathcal{J}_s \ell_1)^{-1} \Gamma_s^* + \mathcal{J}_v [\ell_1 (\mathcal{J} - \mathcal{J}_s \ell_1)^{-1} \mathcal{J}_s + \mathcal{J}] \ell_2 \quad (29)$$

4 RESULTS

In the preceding two sections an approximate solution of the spanwise loading equation (2) has been given, which enables the loading to be evaluated at m spanwise collocation points η_v and k discontinuity points η_s ($\eta_s \neq \eta_v$). This solution is, theoretically, an improvement on the earlier method⁵, which assumed that the calculation of the loading at the η_v points is not affected by the defining of the loading at the η_s points, and that at each of these k points, α_{10} may be expressed in terms of the loading at the η_v points and at that discontinuity point only. It was considered that this method would be likely to give increasing errors as the distance between two successive discontinuity points decreased, e.g. diminishing span of a cut-out in a trailing-edge, extended-chord flap.

An example has been worked out to compare the results of the earlier method with those by the method of this Report. Values of lift coefficient, vortex drag coefficient and vortex drag factor have been calculated for a wing of aspect ratio 8.35, taper ratio 0.35, mid-chord angle of sweepback 26.4° and angle of incidence zero. Each half wing had two flaps (see Fig.1), the inner running from the centreline to 50% of the semispan and the outer from 97% to a range of positions between 60% and 50% of the semispan. All flaps extended the local basic chord by 20%, had a chord of 34% of the local extended chord, and were deflected 15° .

The results are shown in Tables 1, 2 and 3. The vortex drag factor K is defined as $K = \pi A C_{D_V} / C_L^2$. Mk.3 and Mk.4 refer, respectively, to versions of a computer program based on the earlier and improved methods of calculating the

spanwise loading. The numbers 31, 33, 45 refer to the value of m used, the number of Multhopp spanwise collocation points. It is immediately obvious that the improved solution has not materially altered the results, at least for this example. In fact, for the lift coefficient it has not been possible to represent the differences on Fig.2. For vortex drag coefficient, Table 2 indicates some small differences and, where possible, these are shown on Fig.3. Extra points are shown on this figure (computed by the earlier method) but are not tabulated, in order to define the curves more exactly in the regions where the curvatures change rapidly. Small differences are also apparent for vortex drag factor (Table 3 and Fig.4).

It is quite clear from these three figures that the effect of m , the number of collocation points, is greater than any improvements gained by the use of the method described in this Report. Each of the three curves shown on Fig.3 has one or more inflexions from a generally smooth curve. The centre of one of these inflexions always corresponds to a spanwise distance between the flaps which makes the inner tip of the outboard flap coincide with a Multhopp collocation point. This situation is tolerated by the earlier method, but with the improved method, leads to singularities in the analysis of section 1 (viz. equation (5)). In the region of one of the inflexions in the curves of Fig.3, convergence between equations (26) and (27) becomes very slow, and the vector γ_s^* cannot be determined very accurately. This leads to a slight amount of 'waviness' in $\gamma(\eta)$ or oscillation about a smooth mean distribution, over the outer parts of the wing. Nevertheless, the differences between the results of the two methods still remain small, and the difficulty cannot explain the reason for the inflexions in the results using the earlier method.

This reason, it is thought, lies in the nature of the numerical method used for integrating the spanwise distributions of γ and $\gamma\alpha_{i0}$ to obtain C_L and C_{Dv} . Fig.5 shows values of $\gamma\alpha_{i0}$ computed using 31, 33 and 45 collocation points, for a gap between the flaps equal to 10% of the semispan. Over the flaps $\gamma\alpha_{i0}$ is positive, but across the gap it is negative. To integrate this function a new distribution is found, which is equal to $\gamma\alpha_{i0}$ plus, at all points η , the sum of the amounts of the discontinuities at points η_s for which $\eta_s > \eta$. Thus, in the example shown on Fig.5, the points between $\eta = 0.5$ and 0.6 are converted to positive values, and some adjustment takes place to the values of $\gamma\alpha_{i0}$ over the inner flap, as the amounts of the

discontinuities at the flap tips are not quite equal and opposite. This adjustment enables a continuous curve to be drawn through all points, as shown on the figure. The integral of $\gamma_{\alpha_{10}}$ over the whole span thus equals the integral of the new curve minus the sum of the products of the amounts of the discontinuities at η_s with $(1 + \eta_s)$.

Across the gap between the flaps the curvature of $\gamma_{\alpha_{10}}$ changes quite rapidly, and just three possible curves are drawn on the figure. The cubic spline method⁶ was used to integrate $\gamma_{\alpha_{10}}$ in the computer program, and a characteristic of spline fitting is that curvatures tend to be minimised. The inflexions in the curves of Figs.3,4 occur where there are changes in the number of points included in the part of the curve across the gap between the flaps. At these places two of the calculation points are almost coincident, thus providing a locally strong constraint on the shape of the fitted curve, but leaving the program a relatively large amount of freedom to fit a curve across the whole of the gap.

Although the inflexions in the curves drawn on Figs.3 and 4 appear to make significant deviations from their general regular trends, it should be noted that the scales used for C_{D_V} and K are very large, and the deviations are, in fact, insignificant. Furthermore, it should be remembered that the linear, small-deflection theory upon which these results are based, is approximate and the values shown on the figures are not physically exact.

There is a further effect which must be considered when choosing the number of collocation points for the calculation. It has been found that the magnitude of the vortex drag factor on swept wings¹¹ is affected by both the parity and actual number of collocation points. Fig.6 shows this effect for wings without flaps, of aspect ratio 8.0, taper ratio 0.8 and angles of sweepback of 0, 15 and 30 degrees. As the angle of sweepback increases, more collocation points are required in order to maintain the same relative accuracy. Fig.7 shows the effect of sweepback on the spanwise load distribution of these wings, all three curves were calculated using $m = 31$. A major effect of sweepback is the loss in lift in the region of the centre of the wing. For the wing sweptback 30° , values of γ at the collocation points for differing m are shown on Fig.8. For m odd, one of the collocation points is on the centreline, so that the minimum value across the centreline is defined exactly. As m increases, the distribution of γ changes quite markedly near the centreline. This effect is also apparent for the distribution of α_{10} , shown on Fig.9. For $\eta > 0.4$, there is very little difference between any of the

curves. Once again, the scale of K used on Fig.6 is very large, so that as long as at least 30, say, collocation points are used, the exact choice is not greatly significant.

5 CONCLUSIONS

A method has been presented for the approximate solution of a version of Prandtl's aerofoil equation for wings with an arbitrary number of discontinuities in chord or geometric angle of incidence. The method is, theoretically, an improvement on an earlier one⁵. A comparison has been made between the results of the two methods, for the example of a sweptback, tapered wing with two extending-chord flaps on each wing-half. For this example, there was no significant improvement in the calculated values of lift and vortex drag coefficients, even for very small gaps between the flaps. However, because of limitations imposed by the numerical methods of the computer versions of the two methods, care has to be taken in the choice of the number of Multhopp collocation points. For a sweptback wing, this number should be odd and as large as possible. Furthermore, it is best to arrange that a collocation point does not come near to coinciding (within 1% of the semispan, say) with a flap tip.

Acknowledgement

Much of the data for Fig.6 was supplied by Mr. D.R. Holt of Hawker Siddeley Aviation Limited, Brough.

Table 1
LIFT COEFFICIENT

| % gap | 31 points | | 33 points | | 45 points |
|-------|-----------|---------|-----------|---------|-----------|
| | Mk. 3 | Mk. 4 | Mk. 3 | Mk. 4 | Mk. 3 |
| 0 | 0.93896 | 0.93896 | 0.93938 | 0.93938 | 0.94083 |
| 1 | 0.92663 | 0.92663 | 0.92742 | 0.92743 | 0.92907 |
| 2 | 0.91482 | 0.91482 | 0.91685 | 0.91703 | |
| 3 | 0.90339 | 0.90338 | 0.90749 | 0.90795 | 0.90772 |
| 4 | 0.89236 | 0.89243 | 0.89621 | 0.89640 | 0.89639 |
| 5 | 0.88197 | 0.88207 | 0.88504 | 0.88512 | 0.88511 |
| 6 | 0.87236 | 0.87249 | 0.87387 | 0.87393 | 0.87395 |
| 7 | 0.86202 | 0.86204 | 0.86278 | 0.86282 | 0.86299 |
| 8 | 0.85156 | 0.85158 | 0.85183 | 0.85185 | 0.85266 |
| 10 | 0.83060 | 0.83060 | 0.83036 | 0.83027 | 0.83251 |

Table 2
VORTEX DRAG COEFFICIENT

| % gap | 31 points | | 33 points | | 45 points |
|-------|-----------|----------|-----------|----------|-----------|
| | Mk. 3 | Mk. 4 | Mk. 3 | Mk. 4 | Mk. 3 |
| 0 | 0.033879 | 0.033879 | 0.033910 | 0.033909 | 0.034002 |
| 1 | 0.033234 | 0.033240 | 0.033232 | 0.033219 | 0.033311 |
| 2 | 0.032730 | 0.032727 | 0.032626 | 0.032611 | |
| 3 | 0.032307 | 0.032307 | 0.031843 | 0.031796 | 0.032227 |
| 4 | 0.031976 | 0.032048 | 0.031620 | 0.031651 | 0.031926 |
| 5 | 0.031731 | 0.031770 | 0.031383 | 0.031424 | 0.031691 |
| 6 | 0.031375 | 0.031416 | 0.031194 | 0.031226 | 0.031515 |
| 7 | 0.031116 | 0.031134 | 0.031054 | 0.031075 | 0.031395 |
| 8 | 0.030906 | 0.030918 | 0.030957 | 0.030970 | 0.031250 |
| 10 | 0.030602 | 0.030606 | 0.030937 | 0.031005 | 0.030814 |

Table 3
VORTEX DRAG FACTOR

| % gap | 31 points | | 33 points | | 45 points |
|-------|-----------|---------|-----------|---------|-----------|
| | Mk.3 | Mk.4 | Mk.3 | Mk.4 | Mk.3 |
| 0 | 1.00814 | 1.00814 | 1.00816 | 1.00815 | 1.00778 |
| 1 | 1.01545 | 1.01565 | 1.01367 | 1.01323 | 1.01248 |
| 2 | 1.02571 | 1.02593 | 1.01827 | 1.01737 | |
| 3 | 1.03856 | 1.03857 | 1.01443 | 1.01189 | 1.02614 |
| 4 | 1.05350 | 1.05571 | 1.03283 | 1.03341 | 1.04241 |
| 5 | 1.07022 | 1.07128 | 1.05112 | 1.05232 | 1.06128 |
| 6 | 1.08162 | 1.08272 | 1.07166 | 1.07263 | 1.08250 |
| 7 | 1.09861 | 1.09918 | 1.09446 | 1.09512 | 1.10596 |
| 8 | 1.11818 | 1.11855 | 1.11931 | 1.11970 | 1.12765 |
| 10 | 1.16374 | 1.16388 | 1.17714 | 1.17999 | 1.16645 |

SYMBOLS

| | |
|--|---|
| a | sectional lift slope |
| b | wing span |
| c | local wing chord |
| k | number of discontinuities in induced angle of incidence |
| m | number of spanwise Multhopp points |
| A_{i0I} | vector of values of angle of incidence induced by the spanwise loading γ_I |
| $F(\vartheta, \vartheta_s)$ | function used to generate γ_I |
| α | geometric angle of incidence |
| α_{i0} | induced angle of incidence on wings of large aspect ratio |
| γ | nondimensional spanwise load distribution |
| $\bar{\gamma}$ | approximation to γ |
| γ_I | load distribution that induces a discontinuous distribution of angle of incidence |
| γ^* | $\gamma - \gamma_I$ |
| ϑ, η | spanwise coordinates, $\eta = \cos \vartheta, \eta \leq 1$ |
| σ_s | jump in the value of the geometric angle of incidence at η_s |
| τ_s | quantity associated with the discontinuity in chord at η_s |
| ω | downwash factor |
| Γ | matrix that couples $\bar{\gamma}_s$ to γ_n |
| Ψ | matrix concerned with the error between $\bar{\gamma}_s$ and γ_s |
| Λ | vector of values of α/ω |
| Υ | vector of values of γ |
| \mathcal{F} | matrix with elements $F(\vartheta, \vartheta_s)$ |
| \mathcal{I} | unit matrix |
| \mathcal{I}_2 | matrix used to evaluate A_{i0Is} |
| \mathcal{L}_1 | matrix formed from τ_s/ω_s |
| \mathcal{L}_2 | vector formed from σ_s/ω_s |
| \mathcal{M} | matrices used in the evaluation of α_{i0} |
| \mathcal{N} | diagonal matrices with elements equal to $2b/\omega ac$ |
| $\mathcal{R}_1, \mathcal{R}_2, \mathcal{R}_3, \mathcal{R}_4$ | matrices of Multhopp coefficients |

SYMBOLS (Contd)

- s, n subscripts denoting evaluation at the discontinuity points and
 Multhopp points, respectively
- *, I suffices denoting a relationship to γ^* and γ_I

REFERENCES

- | <u>No.</u> | <u>Author(s)</u> | <u>Title, etc.</u> |
|------------|------------------|---|
| 1 | D. Kuchemann | A simple method of calculating the span and chordwise loading on straight and swept wings of any given aspect ratio at subsonic speeds. ARC R & M 2935 (1952) |
| 2 | H. Multhopp | Die Berechnung der Auftriebsverteilung von Tragflügeln. <i>Luftfahrtforschung</i> , <u>15</u> , 153-169 (1938). Available as 'The calculation of the lift distribution of aerofoils', translated by M. Flint (ARC 8516) |
| 3 | J. Weissinger | Die Auftriebsverteilung von Tragflügeln mit Tiefensprung. <i>Ingen.-Arch.</i> , <u>20</u> , 166 (1952) |
| 4 | J. Weber | Theoretical load distribution on a wing with vertical plates. ARC R & M 2960 (1954) |
| 5 | J. McKie | The estimation of the loading on swept wings with extending chord flaps at subsonic speeds. ARC CP 1110 (1969) |
| 6 | J.M. Freeland | Cubic spline fitting. RAE Math Computing Note, Series C335 (1965) |

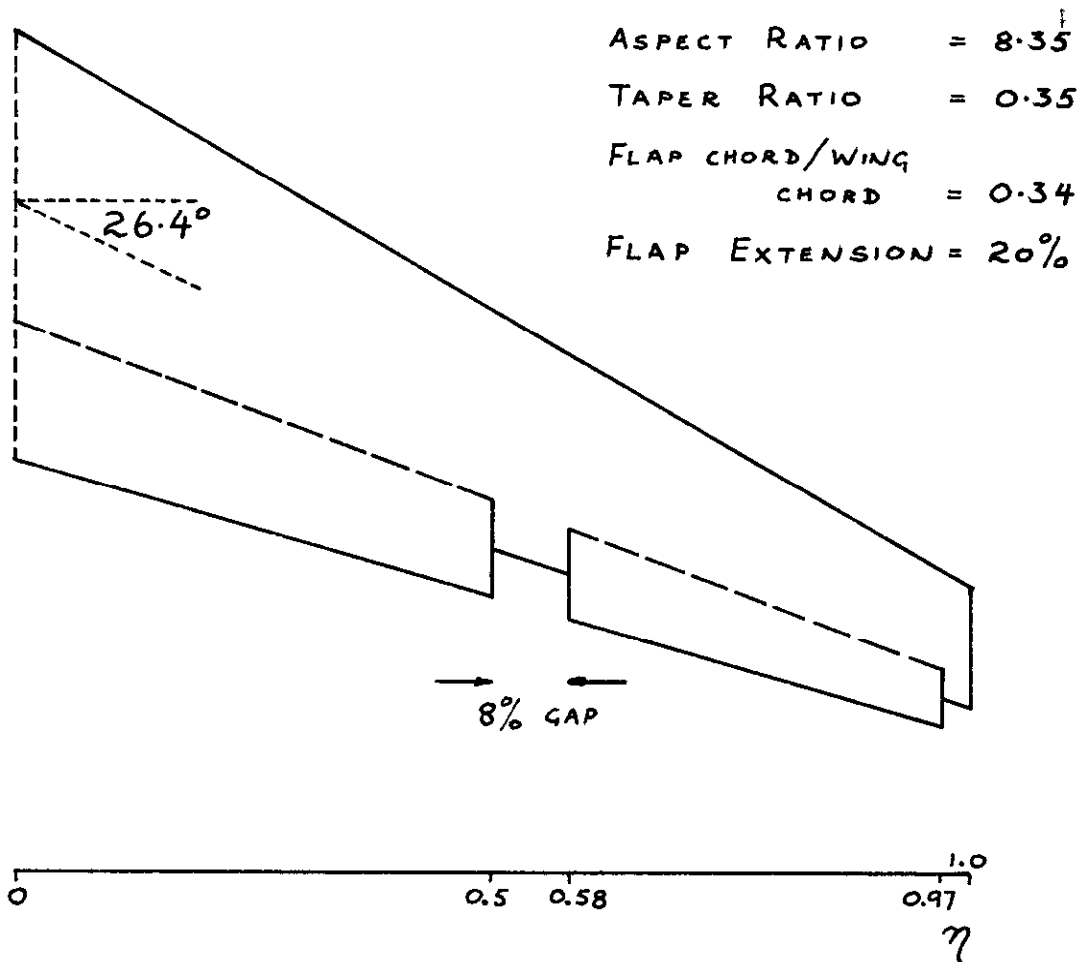


Fig.1 Wing used in example, showing 8% spanwise gap between the flaps

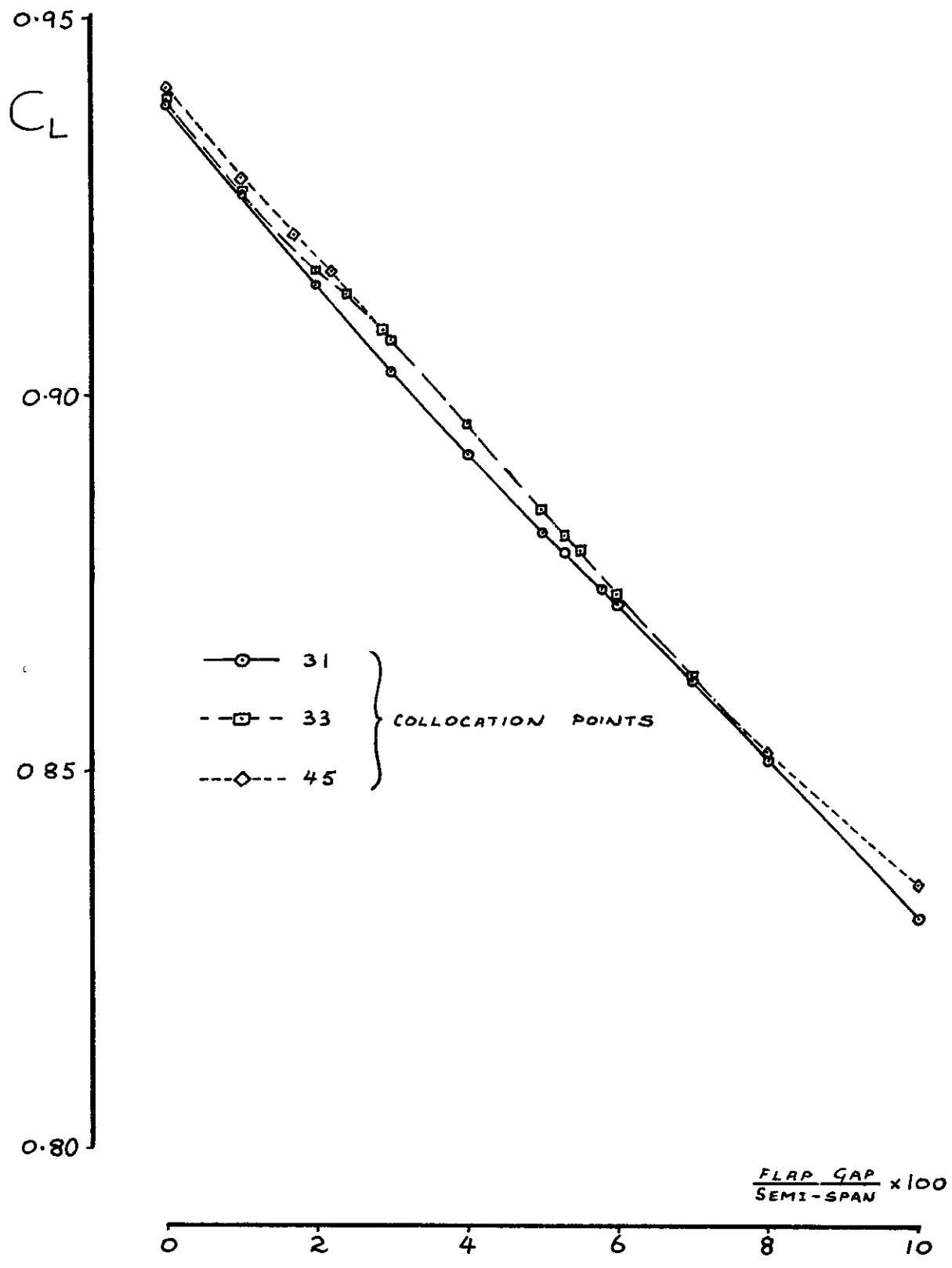


Fig.2 Variation of lift coefficient with span of flap cut-out

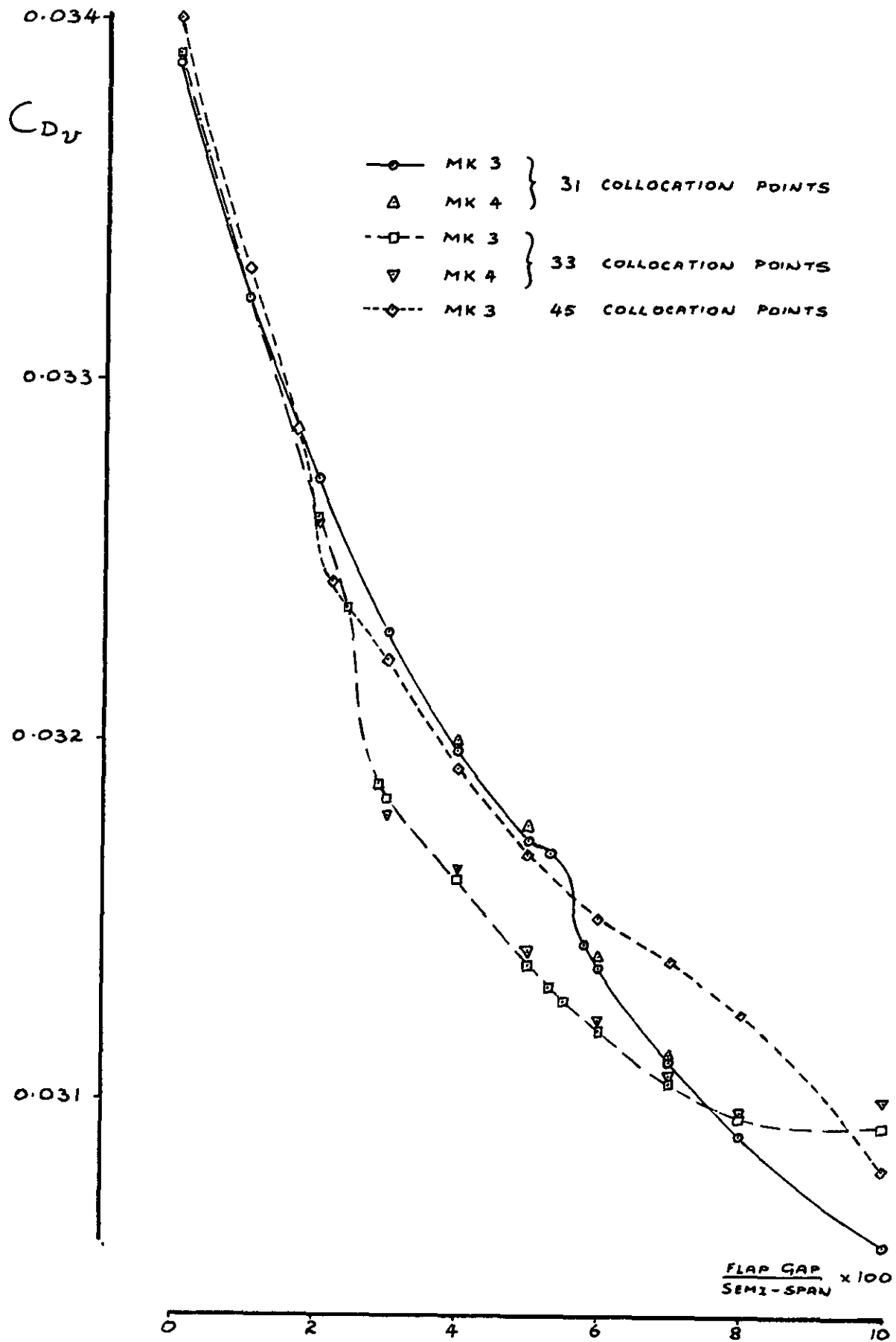


Fig.3 Variation of vortex drag coefficient with span of flap cut-out

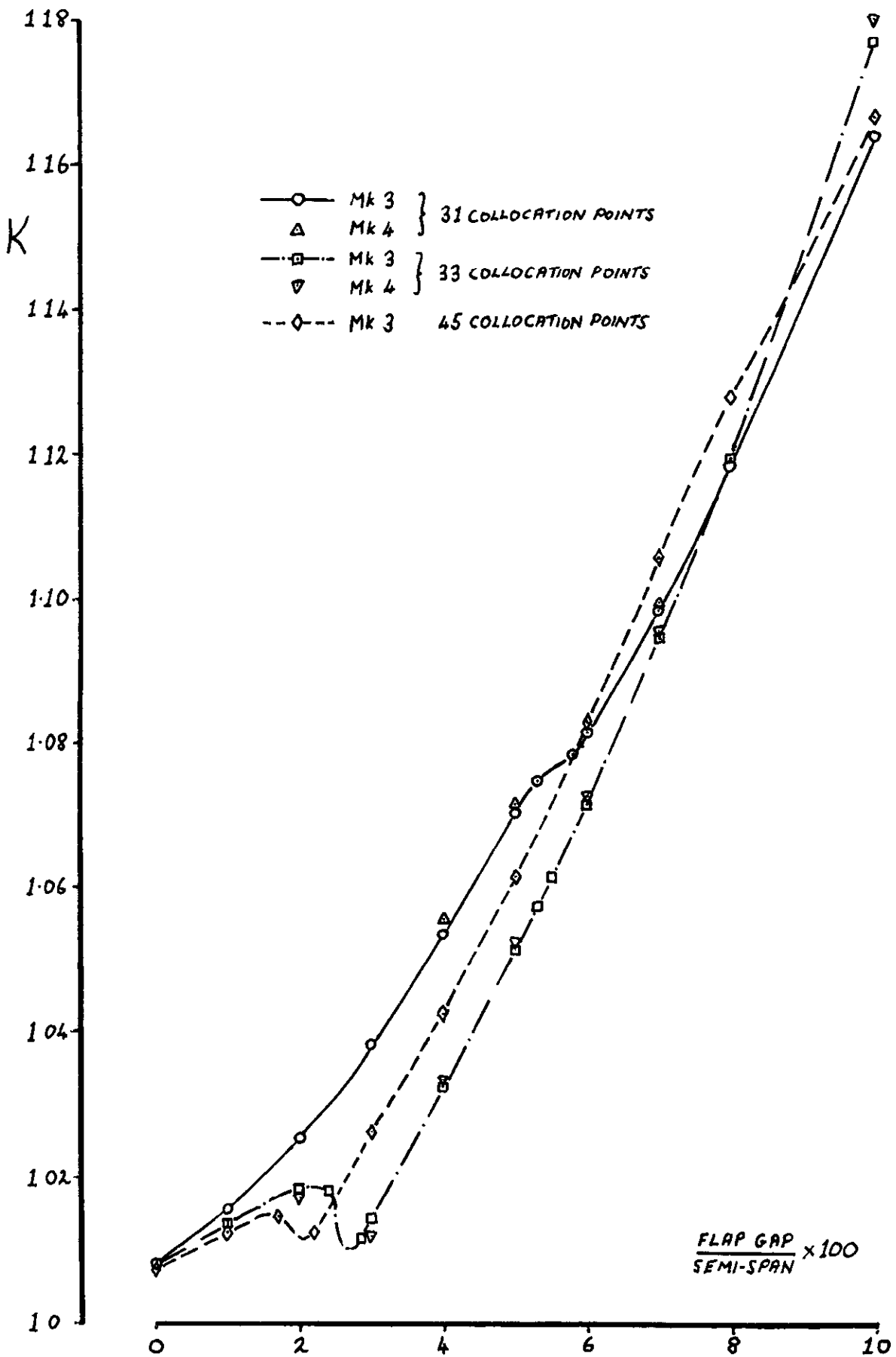


Fig.4 Variation of vortex drag factor with span of flap cut-out

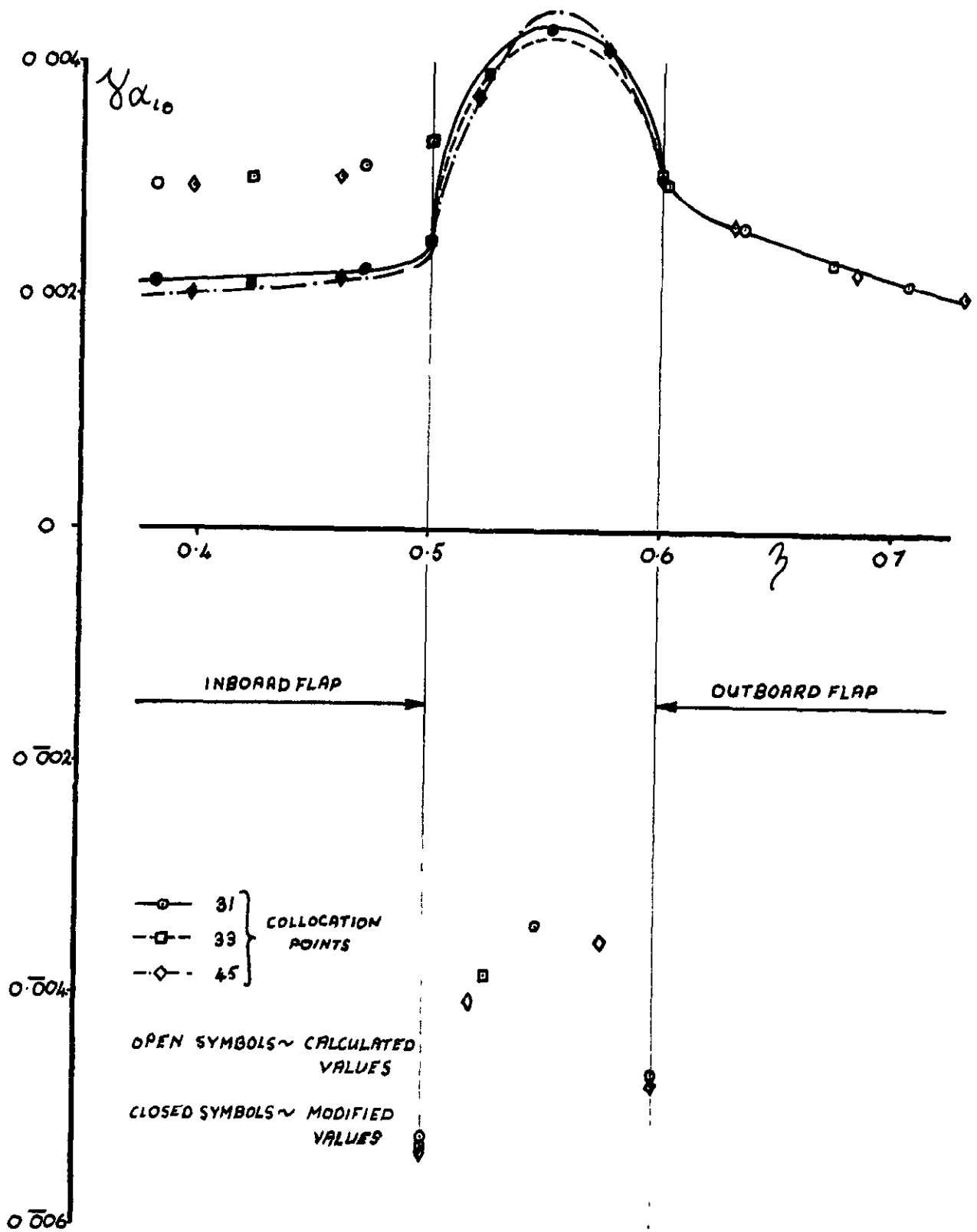


Fig.5 Spanwise variation of $\gamma\alpha_{10}$ near a flap cut-out

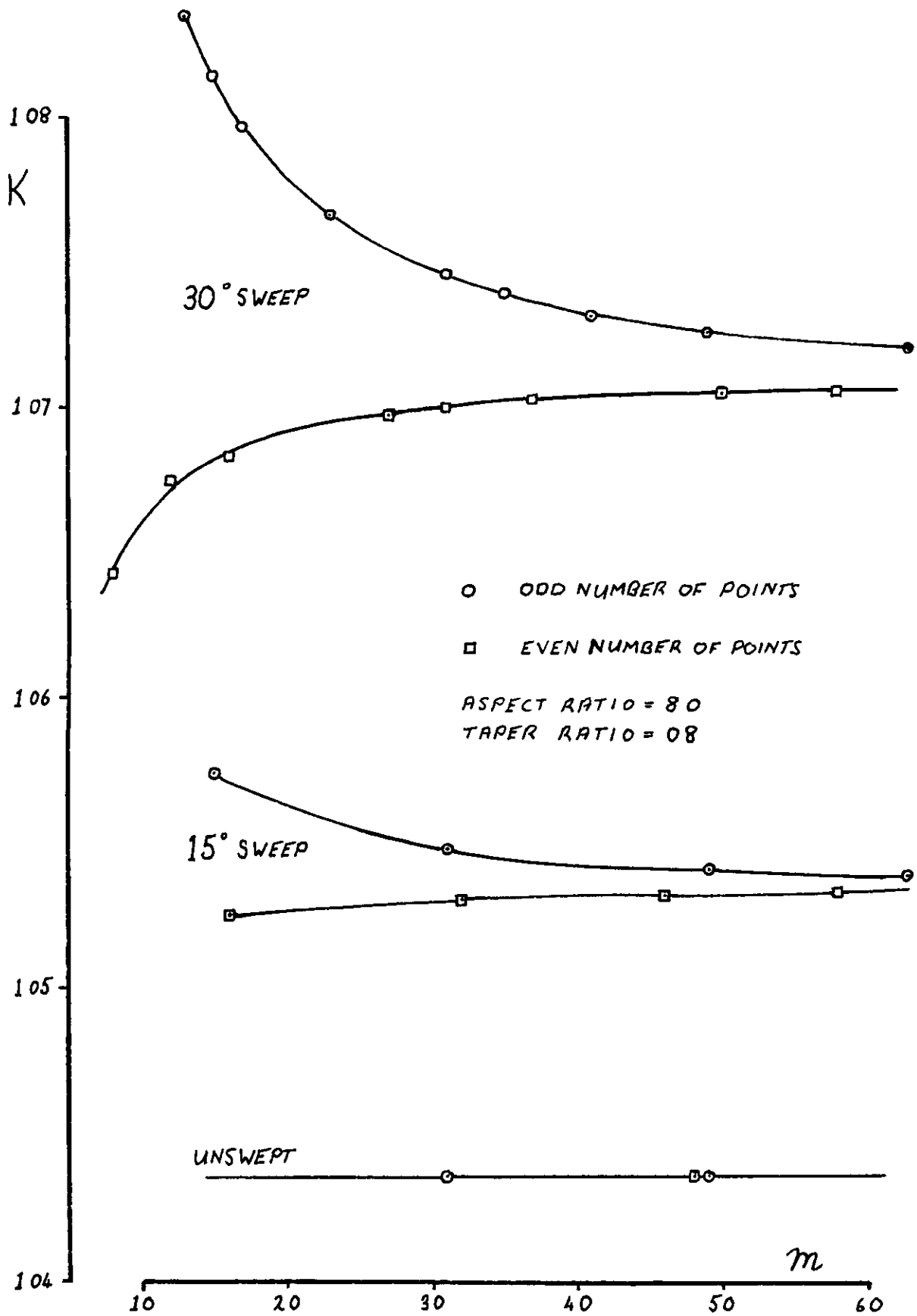


Fig.6 Effect of number of collocation points on vortex drag factors of plain wings

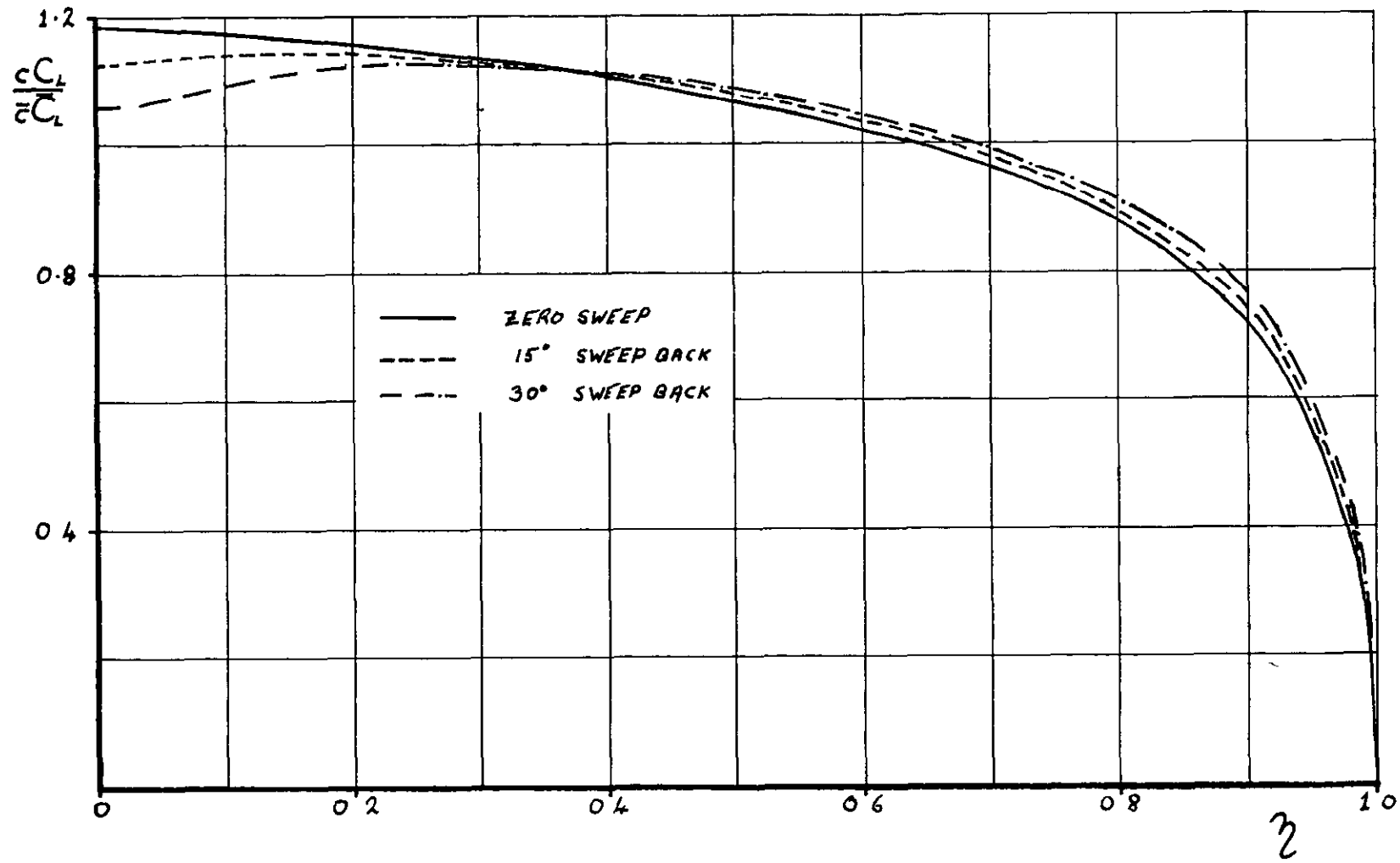


Fig.7 Effect of sweep on the spanwise lift distribution

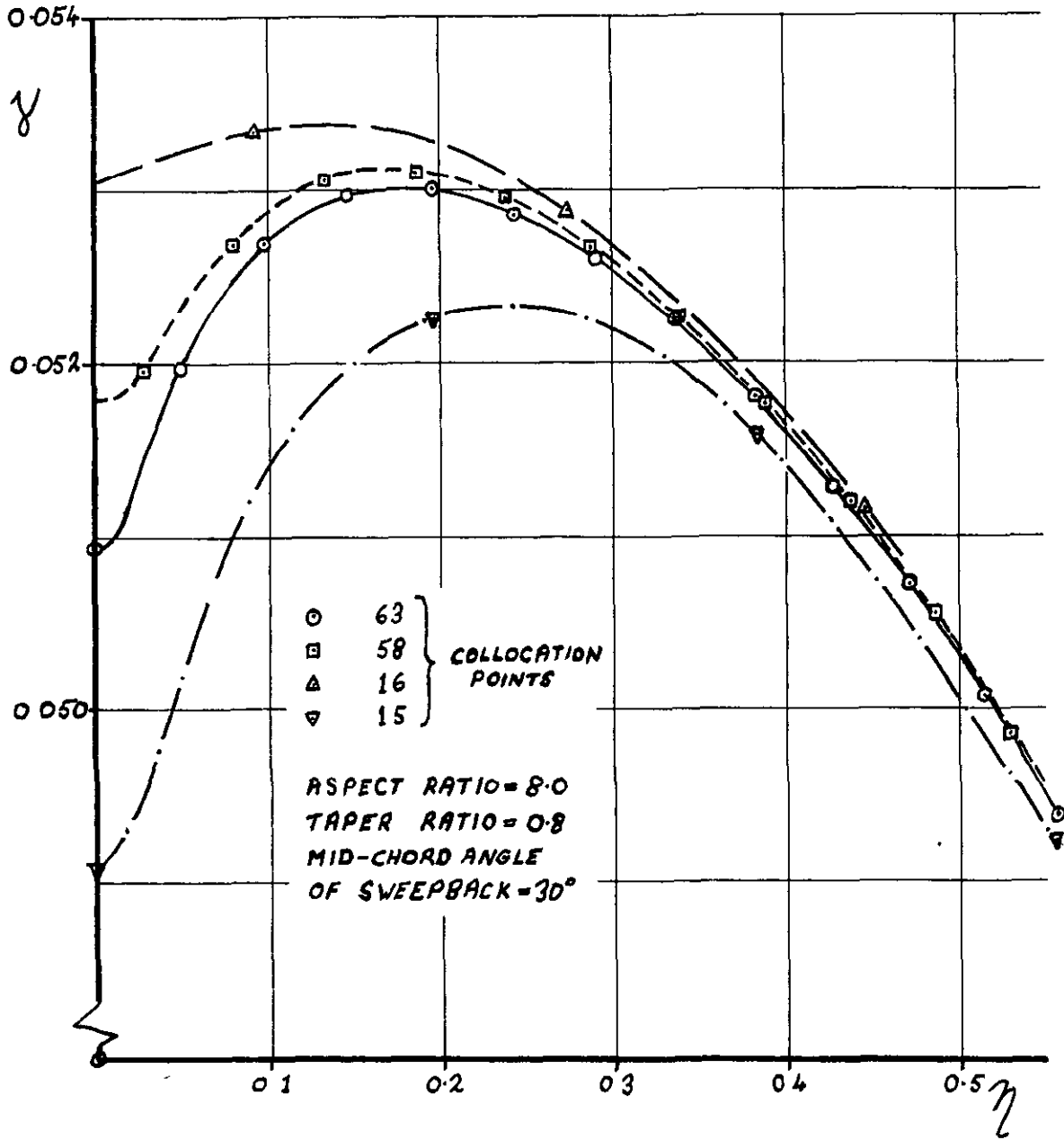


Fig.8 Values of γ at the spanwise collocation points

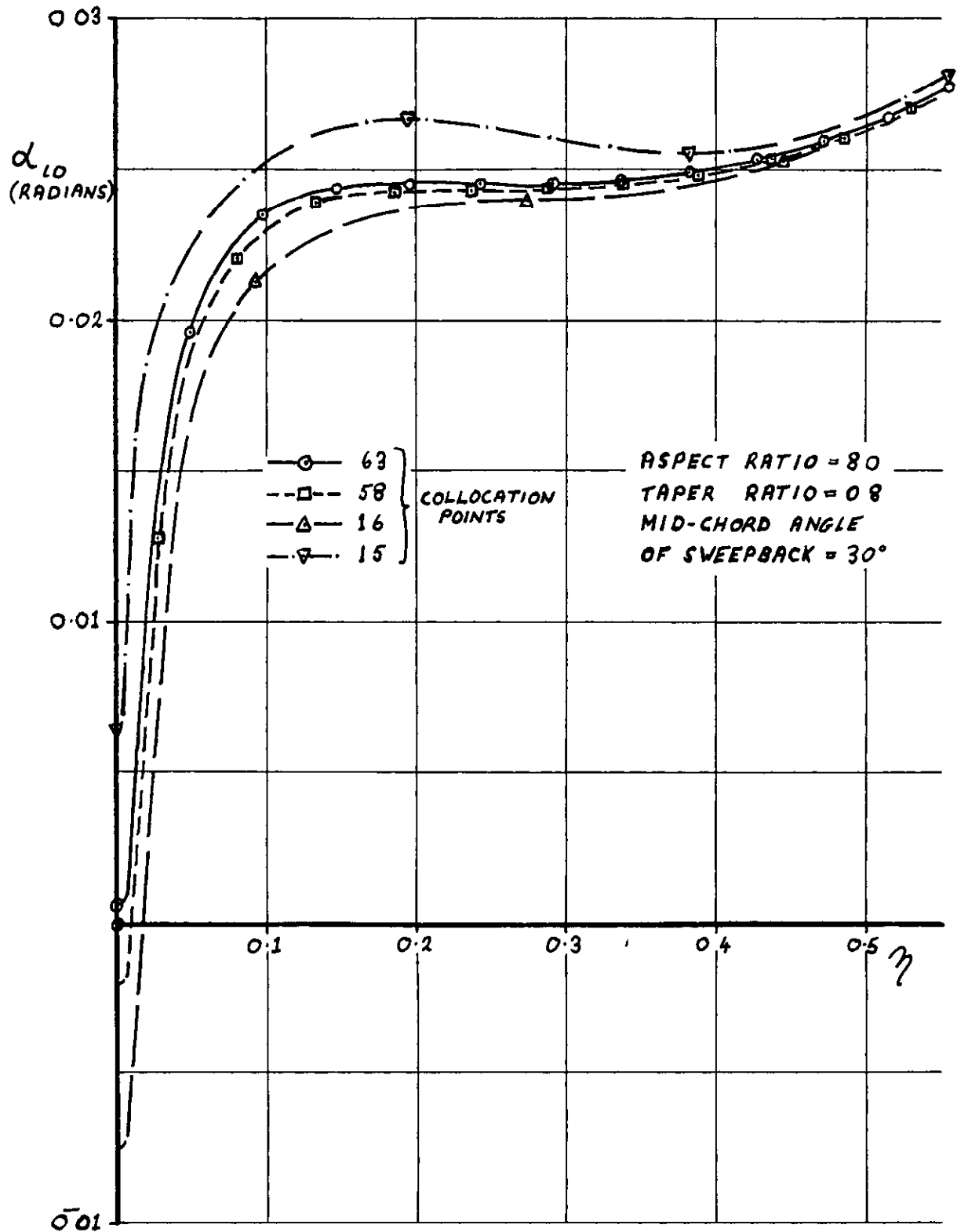


Fig.9 Values of α_{i0} at the spanwise collocation points

Printed in England for Her Majesty's Stationery Office by the Royal Aircraft Establishment, Farnborough Dd 503427 K 4

DETACHABLE ABSTRACT CARD

ARC CP No 1213
September 1971

McKie, J

**SOME MODIFICATIONS TO THE CALCULATION METHOD
FOR WINGS WITH PART-SPAN EXTENDING-CHORD FLAPS
GIVEN IN RAE TECHNICAL REPORT 69034**

A method is given for the approximate solution of a version of Prandtl's aerofoil equation for wings with an arbitrary number of discontinuities in chord or geometric angle of incidence. The method is an attempt to improve on an earlier one given in RAE Technical Report 69034. For the example of a swept wing of large aspect ratio with part-span, extending-chord flaps, the results for lift, drag and vortex-drag factor by the improved method show no significant differences from those calculated by the earlier method. Comments are made on other factors affecting the accuracy of the solution.

533 693 1
533 6 048 1
533 694 511
533 6 011 32
533 6 013 13
533 6 013 127

ARC CP No 1213
September 1971

McKie, J

**SOME MODIFICATIONS TO THE CALCULATION METHOD
FOR WINGS WITH PART-SPAN EXTENDING-CHORD FLAPS
GIVEN IN RAE TECHNICAL REPORT 69034**

A method is given for the approximate solution of a version of Prandtl's aerofoil equation for wings with an arbitrary number of discontinuities in chord or geometric angle of incidence. The method is an attempt to improve on an earlier one given in RAE Technical Report 69034. For the example of a swept wing of large aspect ratio with part-span, extending-chord flaps, the results for lift, drag and vortex-drag factor by the improved method show no significant differences from those calculated by the earlier method. Comments are made on other factors affecting the accuracy of the solution.

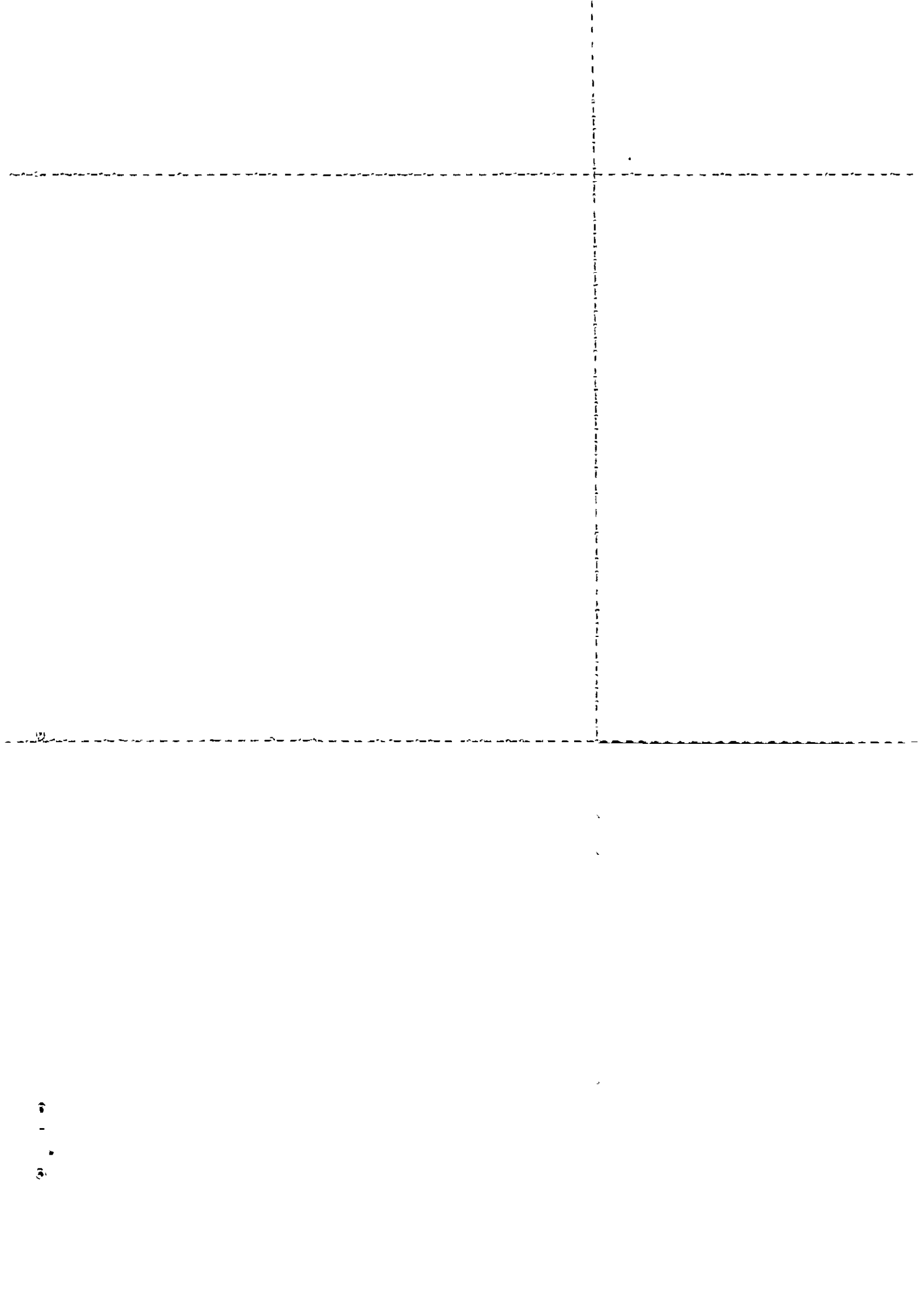
533 693 1
533 6 048 1
533 694 511
533 6 011.32
533 6 013 13
533 6 013 127

A method is given for the approximate solution of a version of Prandtl's aerofoil equation for wings with an arbitrary number of discontinuities in chord or geometric angle of incidence. The method is an attempt to improve on an earlier one given in RAE Technical Report 69034. For the example of a swept wing of large aspect ratio with part-span, extending-chord flaps, the results for lift, drag and vortex-drag factor by the improved method show no significant differences from those calculated by the earlier method. Comments are made on other factors affecting the accuracy of the solution.

**SOME MODIFICATIONS TO THE CALCULATION METHOD
FOR WINGS WITH PART-SPAN EXTENDING-CHORD FLAPS
GIVEN IN RAE TECHNICAL REPORT 69034**

533 693 1
533 6 048 1
533 694 511
533 6 011 32
533 6 013 13
533 6 013 127

ARC CP No 1213
September 1971
McKie, J



© CROWN COPYRIGHT 1972

HER MAJESTY'S STATIONERY OFFICE

Government Bookshops

49 High Holborn, London WC1V 6HB
13a Castle Street, Edinburgh EH2 3AR
109 St Mary Street, Cardiff CF1 1JW
Brazennose Street, Manchester M60 8AS
50 Fairfax Street, Bristol BS1 3DE
258 Broad Street, Birmingham B1 2HE
80 Chichester Street, Belfast BT1 4JY

*Government publications are also available
through booksellers*